

The hydrous components in garnets: Grossular-hydrogrossular

GEORGE R. ROSSMAN, ROGER D. AINES*

Division of Geological and Planetary Science, California Institute of Technology, Pasadena, California 91125, U.S.A.

ABSTRACT

Grossular garnets from 33 localities were examined for indications of OH⁻ or H₂O in their infrared spectrum. All contained OH⁻. Classical hydrogrossular with more than 5 wt% H₂O displays systematic spectroscopic behavior consistent with the hydrogarnet substitution consisting of two absorption bands at 3598 and 3662 cm⁻¹. These spectroscopic characteristics were generally not observed in other grossular samples. Instead, 20 distinct absorption bands have been identified in the spectra of common grossular, occurring in groups of four to ten bands. Both the number and intensities of these bands show a large variation, which does not correspond with the garnet's composition. Seven classes of spectra were identified in the OH region based on the position of the most intense absorption band. The spectroscopic data suggest that in addition to the tetrahedral site, OH groups exist in multiple other environments. The OH content of grossular garnets can be obtained from infrared spectra using the equation $\text{H}_2\text{O wt\%} = 0.0000786 \times \text{integrated absorbance per cm in the OH region near } 3600 \text{ cm}^{-1}$. The OH content of macroscopic grossular crystals (expressed as weight percent H₂O) ranged from 12.8% down to less than 0.005%. Macroscopic grossular typically contains less than 0.3 wt% H₂O. Grossular from rodingites and low-temperature alteration vugs contained much more than that from skarn or contact metamorphic environments.

INTRODUCTION

The hydrogarnet substitution, $(\text{OH})_4 = \text{SiO}_4$, has been established in both synthetic and natural garnets. Grossular analyses have been reported with over 10% H₂O, and the structure of hydrogrossular has been determined with both X-ray and neutron diffraction (Cohen-Addad et al., 1967; Foreman, 1968; Basso et al., 1983; Sacerdoti and Passaglia, 1985; Lager et al., 1987a, 1989). Most hydrogrossular with high OH contents consists of crystals typically no more than a few tens of micrometers in size, often with cores of grossular or intimately admixed with vesuvianite (Zabinski, 1966; Rinaldi and Passaglia, 1989). Although such high H₂O content garnets are rare, previous infrared spectra of macroscopic garnets have indicated that a minor OH component is present in a variety of garnets (Wilkins and Sabine, 1973). We have previously reported the results of a survey of the infrared spectroscopy of a number of pyrope-almandine garnets (Aines and Rossman, 1985a, 1985b) in which nearly all contained OH. The position of the bands in the spectrum of these garnets varied systematically with the garnet composition, but the amount of OH varied for garnets from different localities.

This paper is primarily concerned with the OH content of common, macroscopic garnets of the grossular com-

position. Because the hydrogarnet substitution should be more prevalent in grossular than in pyrope-almandine garnets (Lager et al., 1989), we have examined a number of grossular samples from a variety of localities to determine if the hydrogrossular substitution was, indeed, commonplace and to attempt to quantify the extent of this substitution.

Infrared spectra have often been used previously to characterize synthetic hydrogrossular samples. These spectra confirm that OH is present in hydrogrossular and should be a standard of comparison for the identification of OH in natural samples. However, when Passaglia and Rinaldi (1984) described katoite, a mineral in the hydrogrossular series with less than one-third of the tetrahedral sites occupied by Si, they presented an infrared spectrum that bears little resemblance to previously published grossular spectra and differs in detail from the spectra of synthetic hydrogrossular. Consequently, it seemed appropriate first to examine carefully the spectroscopic properties of garnets with known hydrogrossular substitution in order to compare the spectroscopic properties of natural hydrogrossular samples to their synthetic counterparts and to the common low OH-content grossular samples. Such a comparison has not been previously critically performed.

EXPERIMENTAL DETAILS

Samples were obtained primarily from museums and private collections. Details of samples, localities, and major element compositions are presented in Tables 1 and

* Present address: Department of Earth Science, Lawrence Livermore National Laboratories, Livermore, California 94550, U.S.A.

TABLE 1. Grossular garnet samples

| Number | Variety | Locality | Class | Abs/mm |
|--------|-----------------|-----------------------------------------------------|-------|--------|
| 42 | orange-brown | [McFall mine?], calcite skarn, Ramona, CA, U.S.A. | 2 | 4.6 |
| 52 | orange-brown | [Vesper Peak?], WA, U.S.A. | 5 | 2.7 |
| 53 | pale orange | Asbestos, Quebec, Canada | 3, 4 | 4.8 |
| 227 | green tsavorite | Campbell Bridges mine, Tsavo National Park, Kenya | 2b | 1.8 |
| 229 | green tsavorite | stream gravel, Kenya | 2b | 3.7 |
| 771 | colorless | Meralini Hills, Tanzania | 2b | 3.4 |
| 936 | orange | Bric Camula, Cogoleto, Liguria, Italy | 6 | 22.1 |
| 937 | dark red-orange | Passo del Faiallo, Genova Province, Liguria, Italy | 6 | 13.7 |
| 938 | dark red-brown | Ossola Valley, Italy | 5 | 1.5 |
| 941 | pink jade | Buffelsfontein, Rustenberg, S. Africa | 4 | 89.7 |
| 946 | brown-red | Auerbach, Germany | 7 | 4.8 |
| 1037 | orange | Dos Cabezas, Imperial County, CA, U.S.A. | 2b | 1.4 |
| 1038 | green | Jeffrey Mine, Asbestos, Quebec, Canada | 5 | 1.5 |
| 1042 | orange-brown | Vesper Peak, WA, U.S.A. | 5 | 2.8 |
| 1051 | pale orange | [Belvidere Mtn?], Eden Mills, VT, U.S.A. | 3 | 1.0 |
| 1058 | — | synthetic Lager et al. (1989) | 1 | powder |
| 1059 | — | synthetic Lager et al. (1987a) | 1 | powder |
| 1113 | brown-orange | North Hill, Riverside County, CA, U.S.A. | 7 | 1.7 |
| 1122 | orange-brown | [Commercial Quarry?], Crestmore, CA, U.S.A. | 7 | 2.7 |
| 1124 | colorless | Chihuahua, Mexico | 3 | 2.1 |
| 1125 | colorless | Lake Jaco, Mexico | 3, 7 | 0.7 |
| 1129 | pale orange | Belvidere Mountain, VT, U.S.A. | 3 | 3.2 |
| 1131 | black zone | Lake Jaco, Mexico | 3 | 0.2 |
| 1198 | green jade | Transvaal, S. Africa | 4 | 68.3 |
| 1326 | orange | Ala Valley, Piedmont, Italy | 5 | 7.2 |
| 1327 | orange | Sciarborosca, Liguria, Italy | 5 | 6.9 |
| 1329 | massive vein | Commercial Quarry, Crestmore, CA, U.S.A. | 1 | 160.9 |
| 1357 | orange-red | Bric Canizzi, Liguria, Italy | 5 | 20.5 |
| 1358 | colorless | Commercial Quarry, Crestmore, CA, U.S.A. | 1 | 138.5 |
| 1359 | red-orange | Iron gabbro metaroddingite, Gruppo di Voltri, Italy | 4 | 3.4 |
| 1360 | orange | Basaltic metaroddingite, Voltri Massif, Italy | 5 | 15.9 |
| 1364 | massive gray | Maungatapu Survey District, Nelson, New Zealand | 4 | 90.0 |
| 1409 | red-brown | calcite, skarn, Saline Valley, Darwin, CA, U.S.A. | 2, 2b | 5.5 |
| 1411 | birefringent | skarn, Munam, North Korea | 6 | 1.2 |
| 1412 | brown | Mul-Kum mine, South Korea | — | 1.0 |
| 1413 | pale green | Vilyi River, Siberia, U.S.S.R. | 1 | 0.0 |
| 1419 | pale orange | Minot Ledge, Minot, ME, U.S.A. | 2b | 3.2 |
| 1420 | brown | Rauris, Salzburg, Austria | 2 | 8.3 |
| 1422 | brown | Wakefield, Ontario, Canada | 2b | 0.3 |
| 1423 | red-brown | Mountain Beauty mine, Oak Grove, CA, U.S.A. | 7 | 0.6 |
| 1424 | orange | Garnet Queen mine?, Santa Rosa Mtns, CA, U.S.A. | 7 | 3.1 |
| 1427 | massive yellow | Mavora Lakes, Otago, South Island, New Zealand | 4 | — |
| 1429 | red-brown | Essex County, NY, U.S.A. | 7 | 0.6 |
| 1430 | orange | Eden Mills, VT, U.S.A. | 3 | 1.1 |
| 1444 | katoite | Pietramassa, Viterbo, Italy | 1 | powder |

Note: Question mark denotes additional locality information that was not part of the documentation provided with the sample but that we added based on our inspection of the sample. Absorbance per mm refers to the strongest band in the OH region. Integrated intensity in the OH region generally closely follows this parameter. Class refers to the class of spectra in the OH region discussed in text. Multiple numbers mean that different crystals from the same locality have different behavior or that different zones of the crystal show different behavior.

2. The infrared spectra of the natural crystals were obtained from doubly polished single crystals. Exceptions were the fine-grained, massive hydrogarnet samples (nos. 1329, 1364, and 1427), which were studied as doubly polished polycrystalline slabs, and katoite (no. 1444) and the fine-grained powders of synthetic hydrogarnet samples, which were studied as KBr pellets. Details of sample preparation are the same as described in Aines and Rossman (1985a). Details of spectrophotometer measurements are generally the same as described in Aines and Rossman with the exception that most spectra were acquired with a Nicolet 60SX FTIR with an InSb detector at 2 cm⁻¹ resolution. This instrument allowed regions in the sample as small as 25 μm in diameter to be studied selectively. Garnet analyses were performed by electron microprobe as described in Aines and Rossman using

both a MAC5 (Bence-Albee corrections) and JEOL 733 instruments (CITZAF corrections).

Batches of both Ca₃Al₂(O₄H₄)₃ and Ca₃Al₂(SiO₄)_{2.28}(O₄H₄)_{0.72} were provided by G. A. Lager. Ca₃Al₂(O₄D₄)₃ that contained some residual H and was used in the neutron structural refinement of Lager et al. (1987a) was also examined. The position and full width at half height of the band in the OH region of its spectrum are essentially identical to that of Ca₃Al₂(O₄H₄)₃.

RESULTS

Synthetic hydrogrossular

Hydrogarnet of the composition Ca₃Al₂(OH)₁₂ has been synthesized by a number of authors who have also reported its infrared spectrum (Zabinski, 1966; Cohen-Ad-

TABLE 2. Grossular analyses: formula proportions

| Number | Ca | Mg | Fe ²⁺ | Mn | Al | Fe ³⁺ | Cr | V | Ti | Si | H | Infrared wt% H ₂ O |
|---------------------|------|------|------------------|------|------|------------------|------|------|------|------|-------|----------------------------------|
| 42 | 2.89 | 0.00 | 0.08 | 0.01 | 1.89 | 0.11 | 0.00 | na | 0.00 | 3.02 | na | 0.10 |
| 52 | 3.03 | 0.00 | 0.00 | 0.05 | 1.67 | 0.30 | 0.00 | na | 0.02 | 3.00 | na | 0.14 |
| 53 | 2.93 | 0.00 | 0.03 | 0.04 | 1.96 | 0.06 | 0.00 | na | 0.00 | 2.98 | na | 0.21–0.38 |
| 227 | 2.99 | 0.05 | 0.00 | 0.07 | 1.78 | 0.01 | 0.01 | 0.07 | 0.02 | 2.96 | na | 0.09 |
| 229 | 2.99 | 0.05 | 0.00 | 0.05 | 1.84 | 0.00 | 0.02 | na | 0.02 | 3.01 | na | 0.15 |
| 771 | 2.95 | 0.04 | 0.00 | 0.01 | 1.97 | 0.01 | 0.00 | 0.01 | 0.02 | 2.99 | na | 0.18 |
| 936 | 2.92 | 0.00 | 0.08 | 0.00 | 1.05 | 0.84 | 0.00 | 0.00 | 0.11 | 2.99 | na | 1.26 |
| 937 | | | | | | | | | | | | 1.01 |
| 938 | 2.78 | 0.02 | 0.03 | 0.18 | 1.60 | 0.37 | 0.00 | 0.00 | 0.03 | 2.96 | na | 0.08 |
| 941 | | | | | | | | | | | 5.00 | — |
| 946 | 2.85 | 0.01 | 0.13 | 0.01 | 1.66 | 0.25 | 0.00 | 0.01 | 0.01 | 2.97 | na | 0.26 |
| 1037 | 2.90 | 0.01 | 0.08 | 0.01 | 1.78 | 0.20 | 0.00 | 0.01 | 0.01 | 3.01 | na | 0.06 |
| 1038 | 2.96 | 0.00 | 0.05 | 0.07 | 1.93 | 0.04 | 0.02 | na | 0.01 | 3.01 | na | 0.08–0.19 |
| 1042 | | | | | | | | | | | | 0.11–0.13 |
| 1051 | 2.98 | 0.00 | 0.01 | 0.01 | 1.33 | 0.68 | 0.00 | na | 0.00 | 2.98 | na | 0.02–0.04 |
| 1058 ^A | 3.00 | na | na | na | 2.00 | na | na | na | na | 2.28 | 2.86 | — |
| 1059 ^A | 3.00 | na | na | na | 2.00 | na | na | na | na | 0.00 | 12.00 | — |
| 1113 | 2.86 | 0.01 | 0.11 | 0.01 | 1.52 | 0.43 | 0.00 | na | 0.05 | 2.99 | na | 0.09 |
| 1122 | 2.91 | 0.00 | 0.06 | 0.02 | 1.55 | 0.44 | 0.00 | na | 0.02 | 2.99 | na | 0.13 |
| 1124 | 2.95 | 0.06 | 0.00 | 0.01 | 1.93 | 0.05 | 0.00 | 0.00 | 0.00 | 3.02 | na | 0.11 |
| 1125 ^B | 2.98 | 0.05 | 0.00 | 0.01 | 1.70 | 0.24 | 0.00 | na | 0.02 | 2.99 | na | 0.03 |
| 1125 ^C | 3.01 | 0.12 | 0.00 | 0.01 | 1.29 | 0.48 | 0.00 | na | 0.28 | 2.80 | na | 0.04 |
| 1129 | 2.93 | 0.00 | 0.06 | 0.01 | 1.85 | 0.17 | 0.00 | 0.00 | 0.00 | 2.97 | na | 0.17 |
| 1131 | 2.95 | 0.09 | 0.00 | 0.01 | 1.76 | 0.14 | 0.00 | 0.00 | 0.05 | 3.00 | na | 0.01 |
| 1198 | | | | | | | | | | | | 3.59 |
| 1326 | 2.86 | 0.04 | 0.09 | 0.01 | 1.74 | 0.25 | 0.00 | 0.00 | 0.02 | 3.00 | na | 0.37 |
| 1327 | 2.74 | 0.03 | 0.20 | 0.03 | 1.66 | 0.29 | 0.00 | 0.00 | 0.05 | 2.99 | na | 0.47 |
| 1329 ^D | 3.00 | na | na | na | 2.00 | na | na | na | na | 1.64 | 5.43 | — |
| 1357 ^A | 2.67 | 0.16 | 0.14 | 0.02 | 0.99 | 0.80 | 0.00 | na | 0.21 | 2.84 | 0.63 | — |
| 1358 ^{A,D} | 3.00 | na | na | na | 2.00 | na | na | na | na | 1.53 | 5.88 | — |
| 1359 | 2.05 | 0.03 | 0.90 | 0.02 | 1.80 | 0.16 | 0.00 | 0.01 | 0.03 | 2.96 | na | 0.28 |
| 1360 | 2.87 | 0.02 | 0.09 | 0.02 | 1.47 | 0.48 | 0.00 | 0.00 | 0.05 | 2.88 | na | 0.85 |
| 1409 ^E | 2.49 | 0.01 | 0.09 | 0.41 | 1.41 | 0.57 | 0.00 | 0.01 | 0.01 | 2.97 | na | 0.20 |
| 1409 ^F | 2.88 | 0.00 | 0.04 | 0.08 | 1.54 | 0.44 | 0.00 | 0.00 | 0.02 | 3.00 | na | 0.17 |
| 1411 | 2.92 | 0.01 | 0.03 | 0.04 | 1.27 | 0.68 | 0.00 | 0.00 | 0.05 | 2.97 | na | 0.08 |
| 1412 ^A | 2.85 | | | 0.15 | 2.00 | | | | | 3.00 | | 0.10 |
| 1413 | 2.91 | 0.07 | 0.02 | 0.01 | 1.71 | 0.27 | 0.00 | 0.00 | 0.02 | 2.98 | na | 0.0003 |
| 1419 | 2.85 | 0.01 | 0.12 | 0.01 | 1.86 | 0.11 | 0.00 | 0.00 | 0.03 | 2.96 | na | 0.16 |
| 1420 | 2.85 | 0.01 | 0.12 | 0.03 | 1.60 | 0.38 | 0.00 | 0.00 | 0.02 | 2.95 | na | 0.26 |
| 1422 | 2.91 | 0.08 | 0.00 | 0.01 | 1.87 | 0.08 | 0.00 | 0.00 | 0.04 | 2.96 | na | 0.02 |
| 1423 | 2.12 | 0.01 | 0.59 | 0.28 | 1.88 | 0.10 | 0.00 | 0.01 | 0.01 | 2.99 | na | 0.06 |
| 1424 | 2.83 | 0.00 | 0.13 | 0.03 | 1.72 | 0.24 | 0.00 | 0.00 | 0.04 | 2.96 | na | 0.17 |
| 1429 | 2.79 | 0.02 | 0.18 | 0.01 | 1.70 | 0.28 | 0.00 | 0.00 | 0.02 | 2.91 | na | 0.05 |
| 1430 | 2.86 | 0.00 | 0.12 | 0.02 | 1.89 | 0.10 | 0.00 | 0.00 | 0.00 | 3.00 | na | 0.06 |
| 1444 ^A | 2.93 | 0.00 | | | 1.97 | | | | | 0.64 | 9.44 | — |

Note: The abbreviation na = not analyzed. All other analyses are electron microprobe analyses normalized to five cations in the combined X and Y sites, where Ti⁴⁺ is assigned to the Y site, Fe³⁺ is used to fill the Y site, and the remaining Fe is assigned to Fe²⁺ in the X site. Infrared wt% H₂O values are from the calibration discussed in the text.

^A Literature values: no. 1058 Lager et al. (1989), no. 1059 Lager et al. (1987a), no. 1357 Basso et al. (1981), no. 1358 Basso et al. (1983), no. 1412 Hirai and Nakazawa (1986), no. 1444 Sacerdoti and Passaglia (1985).

^B Colorless rim.

^C Brown inner region.

^D From X-ray cell parameters.

^E Rim.

^F Interior.

dad et al., 1967; Harmon et al., 1982; Kobayashi and Shoji, 1983, 1984). The spectra of these synthetics provide a basis of comparison to the natural garnets. The published spectra are dominated by a major band at 3660 cm⁻¹, with a broader side absorption decreasing in intensity to about 3000 cm⁻¹. The magnitude of the broad absorption varies in the published spectra and contains inflections near 3420 cm⁻¹, which are characteristic of weakly bound H₂O, and frequently present as adsorbed H₂O. To avoid adsorbed H₂O, our Ca₃Al₂(OH)₁₂ was care-

fully dried in a desiccator and made into a KBr pellet that was itself redried after preparation. The spectrum of the pellet, dominated by the major peak at 3662 cm⁻¹, shows essentially no indication of the molecular H₂O contribution at 3420 cm⁻¹ and lacks the extensive tail toward lower energies (Fig. 1).

Also relevant to the discussion of natural, hydrous silicate garnets are the synthetic garnets, which have partial substitution of SiO₄ by (OH)₄. Hsu (1980), Cohen-Addad et al. (1967), and Kobayashi and Shoji (1983, 1984) pre-

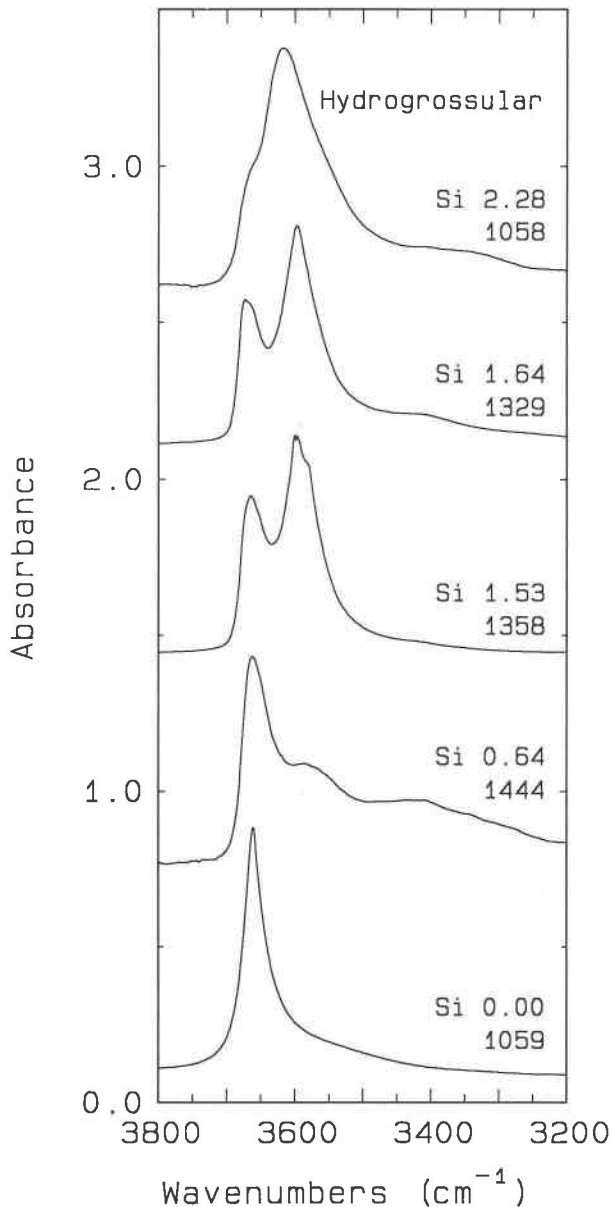


Fig. 1. Comparison of the infrared spectra of natural and synthetic hydrogrossular samples with high OH contents. From top to bottom: synthetic hydrogrossulars, $\text{Ca}_3\text{Al}_2(\text{SiO}_4)_{2.28}(\text{O}_4\text{H}_4)_{0.72}$ (no. 1058) in a KBr pellet; polycrystalline hydrogrossular no. 1329 (4.2 μm thick); single crystal hydrogrossular no. 1358 from Crestmore, California, (5.3 μm thick); katoite (no. 1444) in a KBr pellet; and synthetic $\text{Ca}_3\text{Al}_2(\text{O}_4\text{H}_4)_3$ (no. 1059) dispersed in a KBr pellet.

sented infrared spectra of these materials. They have a major absorption band in the range 3600–3620 cm^{-1} and a minor band near 3660 cm^{-1} . In addition, they show variable amounts of broad absorption near 3420 cm^{-1} , most likely from adsorbed H_2O . Our spectrum of $\text{Ca}_3\text{Al}_2(\text{SiO}_4)_{2.28}(\text{O}_4\text{H}_4)_{0.72}$ is consistent with the published spectra (Fig. 1).

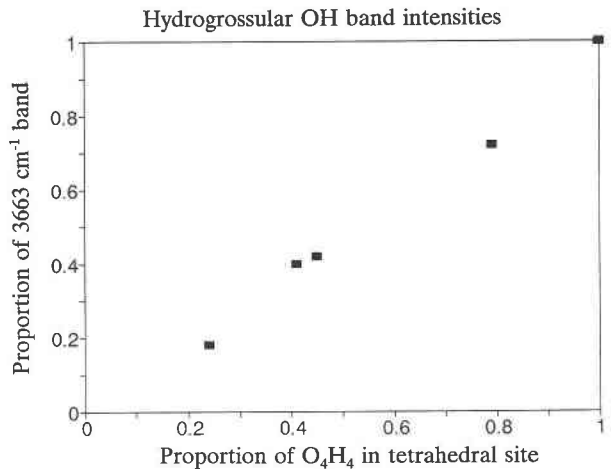


Fig. 2. Correlation between the proportion of the OH intensity in the 3662 cm^{-1} band vs. the proportion of O_4H_4 in the tetrahedral site. The vertical OH intensity axis represents the ratio of band heights defined as $(3662 \text{ cm}^{-1}) / (3662 \text{ cm}^{-1} + 3588 \text{ cm}^{-1})$ where the band heights were estimated by manually fitting the spectrum to two Gaussian bands.

Natural hydrogrossular

Three samples of natural hydrogrossular with extensive OH substitution were examined. One (no. 1358) was the hydrogrossular from Crestmore, California, originally described by Foshag (1920) under the name "plazolite." It is one of the fragments given to Basso by Pabst. Its structure was determined by Pabst (1937) and later refined by Basso et al. (1983). Its composition is approximately $\text{Ca}_3\text{Al}_2(\text{SiO}_4)_{1.53}(\text{OH})_{5.88}$. It consisted of a clear, colorless crystal fragment approximately 600 μm in size. The second sample (no. 1329) from Crestmore, California, originally described as "plazolite?" by Woodward et al. (1941), consists of a colorless, somewhat turbid, fine-grained matrix, 3–5 mm thick, between grains of akermanite. It is from the hand specimen described in the unpublished thesis of R. A. Crippen. The identity of the portion used for spectroscopic measurements was verified by X-ray powder diffraction ($a_0 = 12.15 \text{ \AA}$, which indicates the formula $\text{Ca}_3\text{Al}_2(\text{SiO}_4)_{1.64}(\text{OH})_{5.43}$ according to the calibration of Basso et al., 1983). The third sample is the katoite of Passaglia and Rinaldi (1984). Its spectrum was obtained from a 50- μg crystal cluster that was ground and studied as a micro-KBr pellet.

The infrared spectra of the two Crestmore hydrogrossular samples are similar. They consist of a prominent band at 3598 cm^{-1} with a secondary band at about 3677 cm^{-1} (Fig. 1). The infrared spectra of the macroscopic garnets discussed in the subsequent sections do not look like this.

When the natural and synthetic hydrogrossular samples are compared in Figure 1, some trends appear. The band at 3662 cm^{-1} in the silica-free synthetic garnet is also the dominant band in the katoite spectrum. It is present to

some extent in all the spectra in Figure 1, although it is shifted to slightly higher energies in the spectra of the more silica-rich samples. With increasing silica content, the relative intensity of the band at about 3598 cm^{-1} increases. Our estimate of the proportion of the total OH intensity contained in the 3662 cm^{-1} band, defined as $\text{peak height}_{3662}/(\text{height}_{3662} + \text{height}_{3598})$, is nearly identical to the proportion of (O_4H_4) units in the tetrahedral position, indicating that the two components of the spectrum exhibit simple mixing behavior (Fig. 2).

A different type of spectrum is produced by massive hydrogrossular with much lower OH contents. The best known of these garnets is the so-called pink jade of South Africa, a massive, impure form of hydrogarnet with about 5% H_2O . Both Frankel (1959) and Zabinski (1966) showed an absorption band at about 3620 cm^{-1} in the KBr pellet spectra of pink jade.

Figure 3 compares the spectrum of a single-crystal region in the pink jade from Transvaal (no. 941) with the synthetic $\text{Ca}_3\text{Al}_2(\text{SiO}_4)_2(\text{OH})_4$ (no. 1058). Also included in Figure 3 are the spectra of the massive, pale blue-gray hydrogrossular from Nelson, New Zealand (no. 1364), which is similar to that of the pink jade. The spectrum of the pale yellow massive hydrogrossular from Mavora Lakes, New Zealand (no. 1427), also resembles the pink jade but contains additional features not identifiable with hydrogrossular, presumably arising from other hydrous minerals in the rock. The 3662 cm^{-1} band of the synthetic silica-free hydrogrossular is not prominent in any of these spectra. Although the following discussion will detail the resemblance of the pink jade spectrum to a class of macroscopic grossulars (class 4), the vast majority of grossular spectra do not resemble the spectra of these massive, fine-grained hydrogrossular samples.

Natural macroscopic garnets

Absorption was observed in the OH region of the infrared spectrum of every grossular examined. Only in the spectrum of grossular 1413 was the absorption so weak as to be difficult to obtain. The spectra of these garnet samples show a great diversity, unlike the generally systematic spectral behavior observed in the natural H_2O -rich hydrogrossular and in the pyrope-almandine garnets where the band position varies smoothly with composition (Aines and Rossman, 1985a). The absolute intensity of the OH bands in grossular spans 3 orders of magnitude, significant variation in the appearance of the spectral features occurs within a single crystal, and the number of bands and the positions of bands vary widely among garnets from different localities.

At first, it appears that there is nearly continuous variation among the different types of grossular spectra. However, when a large number of spectra are examined, a number of similarities appear in certain sets of spectra. An empirical classification scheme can be devised based upon the wavelength of the most prominent absorption band in the spectrum. Ultimately, seven such classes of spectra were distinguished. Figure 4 compares the least

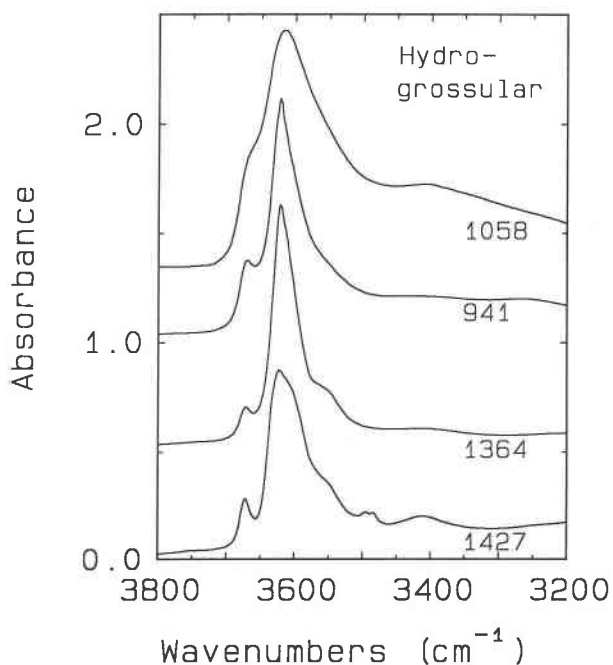


Fig. 3. Comparison of the infrared spectra of natural hydrogrossular and synthetic $\text{Ca}_3\text{Al}_2(\text{SiO}_4)_2(\text{O}_4\text{H}_4)$. From top to bottom: synthetic $\text{Ca}_3\text{Al}_2(\text{SiO}_4)_2(\text{O}_4\text{H}_4)$ no. 1058, pink jade no. 941, massive hydrogrossular no. 1364, and massive hydrogrossular no. 1427. Samples 941 and 1364 are presented scaled to $12\text{-}\mu\text{m}$ thickness. Sample 1427 is scaled to $20\text{ }\mu\text{m}$. The concentration of sample 1058 in the KBr pellet has been arbitrarily adjusted to have an intensity comparable to slabs of the other materials. Spectra have been offset vertically for clarity.

complicated spectrum from each class. These spectra illustrate the range of wavenumbers of peak absorption encountered in grossular; it extends from 3662 cm^{-1} to 3599 cm^{-1} . Figures 5 through 11 illustrate in more detail the individual characteristics observed in these minerals.

Class 1

This group is characterized by the most intense absorption at 3662 cm^{-1} . This is the only band in the spectrum of the synthetic hydrogrossular (no. 1059) and is the most intense band in the katoite spectrum. Only one natural sample has been observed with this band as the dominant band. It is a single zone in the anisotropic grossular (no. FMAP90.111) from the Jeffrey mine (Allen and Buseck, 1988). In anisotropic garnet from Belvidere Mountain, Eden Mills, Vermont, this band may be the most intense in one of the two extinction directions in spectra taken in polarized light.

Class 2

The most prominent band is at 3647 cm^{-1} (Fig. 5). A second feature occurs at 3688 cm^{-1} . Its least complicated representative is the Ramona, California, grossular (no. 42), which occurs in calcite veins (Lager et al., 1987b).

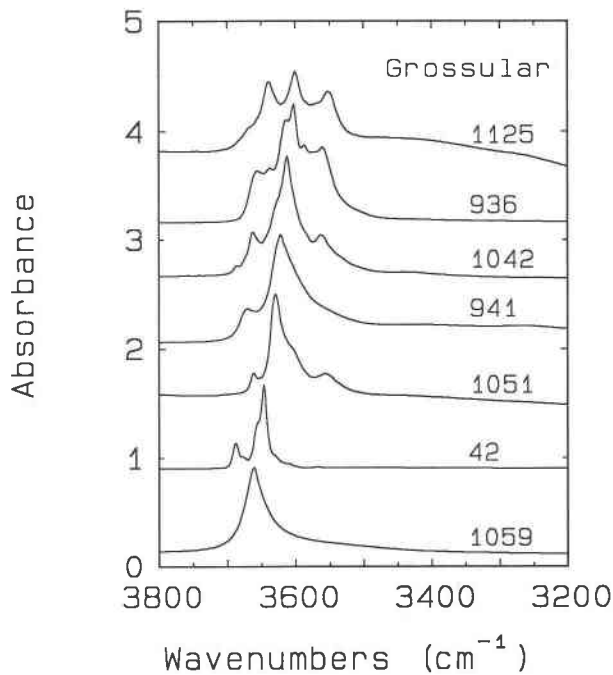


Fig. 4. Comparison of the infrared spectra of the least complicated spectrum from each class of spectra. From bottom to top: class 1 to class 7. Sample numbers are indicated beside each spectral trace. Spectra thicknesses are scaled to produce comparable absorption intensities.

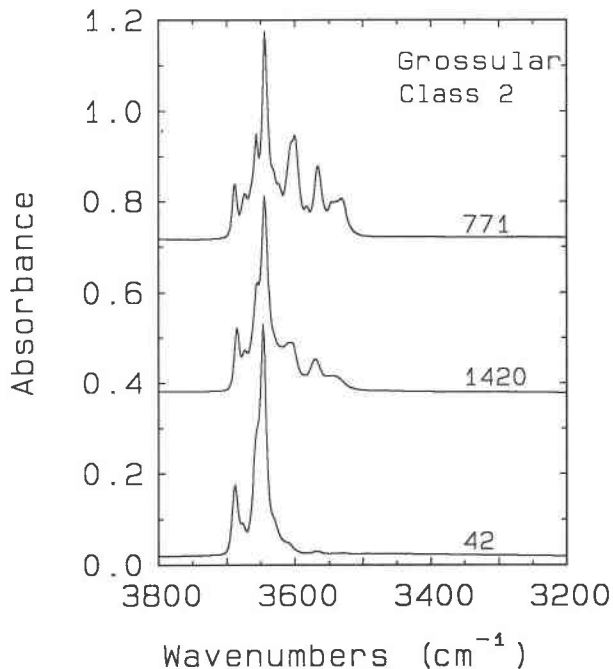


Fig. 5. Class 2 grossular spectra with the strongest peak at 3646 cm^{-1} . From top to bottom: no. 771, $100\text{ }\mu\text{m}$, Tanzania; no. 1420, $54.7\text{ }\mu\text{m}$, Salzburg; no. 42, $94.0\text{ }\mu\text{m}$, Ramona.

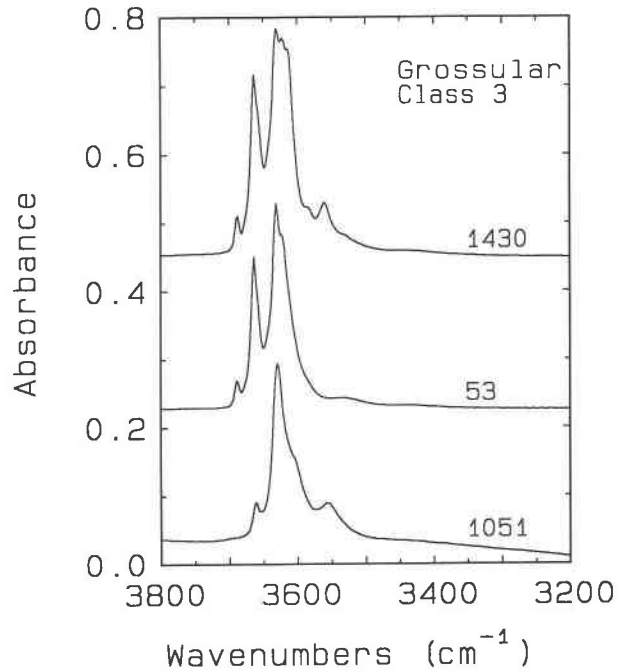


Fig. 6. Class 3 grossular spectra with the strongest peak at 3630 cm^{-1} . From top to bottom: no. 1430, $307\text{ }\mu\text{m}$, Eden Mills; no. 53B-F, $22.1\text{ }\mu\text{m}$, Asbestos; no. 1051, $380\text{ }\mu\text{m}$, Eden Mills.

Class 2b

A more complicated variant of the class 2 garnet consists of garnet with the prominent band at 3645 cm^{-1} in addition to a series of lower energy bands, including those at 3600 , 3568 , and 3548 cm^{-1} . This class is best exemplified by the colorless to bright green vanadian grossular samples from the calcite pods of the Tsavo district of Kenya (nos. 229 and 771).

Class 3

These garnet samples (Fig. 6) have their most prominent component at 3631 cm^{-1} . It is best exemplified by the sample from Eden Mills, Vermont (no. 1051). A component at 3663 cm^{-1} is always present and is sometimes prominent such as in the spectrum of no. 53B. Lower energy bands near 3584 cm^{-1} and 3560 cm^{-1} are well developed in some members of the class.

Class 4

These garnet samples (Fig. 7) have their prominent band at 3621 cm^{-1} . Sample 53 is transitional between groups 3 and 4. The class 3 band at 3631 cm^{-1} is nearly as intense as the 3621 cm^{-1} band. Sample 941 is characteristic of class 4 garnet samples. It is a type of rock known as South African Jade. The pink variety of this material consists of an intimate mixture of two grossular phases that differ in their OH content (Zabinski, 1966; Bank, 1982). Its spectrum has been frequently studied. Both Frankel (1959)

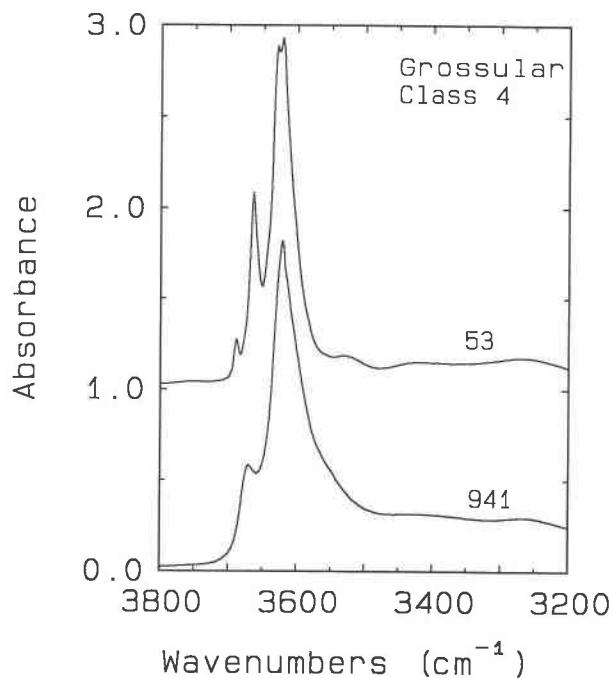


Fig. 7. Class 4 grossular spectra with the strongest peak at 3621 cm^{-1} . From top to bottom: no. 53B, $405\text{ }\mu\text{m}$, Asbestos; no. 941, $21\text{ }\mu\text{m}$, South Africa.

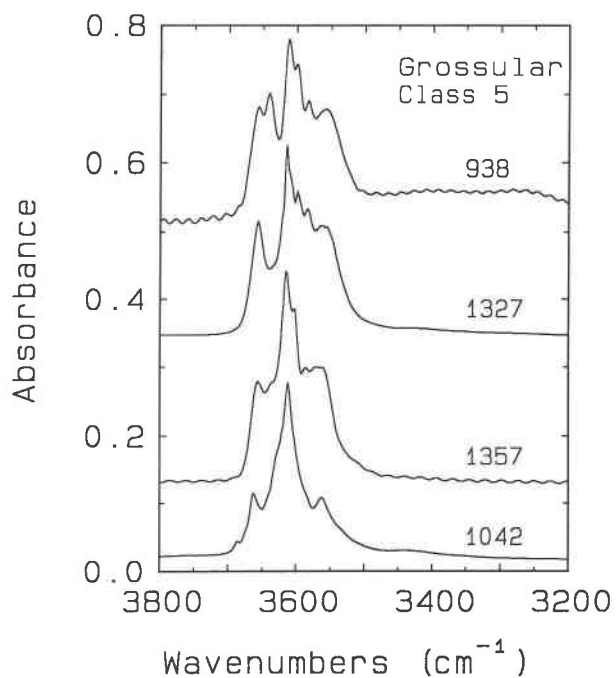


Fig. 8. Class 5 grossular spectra with the strongest peak at 3612 cm^{-1} . From top to bottom: no. 938, $204\text{ }\mu\text{m}$, Ossola Valley; no. 1327, $41\text{ }\mu\text{m}$, Sciara; no. 1357, $38.2\text{ }\mu\text{m}$, Bric Canizzi; no. 1042, $116\text{ }\mu\text{m}$, Vesper Peak.

and Zabinski (1966) showed an absorption band at about 3620 cm^{-1} in a spectrum of the powder from South African Jade. We obtained the spectrum from a small, thin, single grossular crystal in the pink jade. We found a peak at 3621 cm^{-1} and a secondary band at 3672 cm^{-1} . Of all the natural grossular samples, the spectrum of the pink jade most closely resembles the synthetic $\text{Si}_{2.28}$ hydrogarnet (no. 1058), appearing as a spectroscopically better resolved version of the synthetic. The spectra of other, massive hydrogrossular samples from New Zealand resemble the spectra of pink jade (Fig. 3).

Class 5

The class 5 garnet samples were the most commonly encountered (Fig. 8). Their spectra have the strongest peak at 3611 cm^{-1} with side peaks at about 3664 and 3562 cm^{-1} . The spectrum of the Vesper Peak, Washington, garnet (no. 1042) is the simplest in this class. A variety of other peaks can occur in these spectra, primarily between the two side peaks. The Italian grossular samples (e.g., nos. 1327 and 1357) are typical of the more complicated behavior in this class.

Class 6

These grossular samples have their main peak at 3602 cm^{-1} (Fig. 9). Members of this class were infrequently encountered. The distinction between classes 6 and 7 is small. Grossular 1411 is transitional between the two classes.

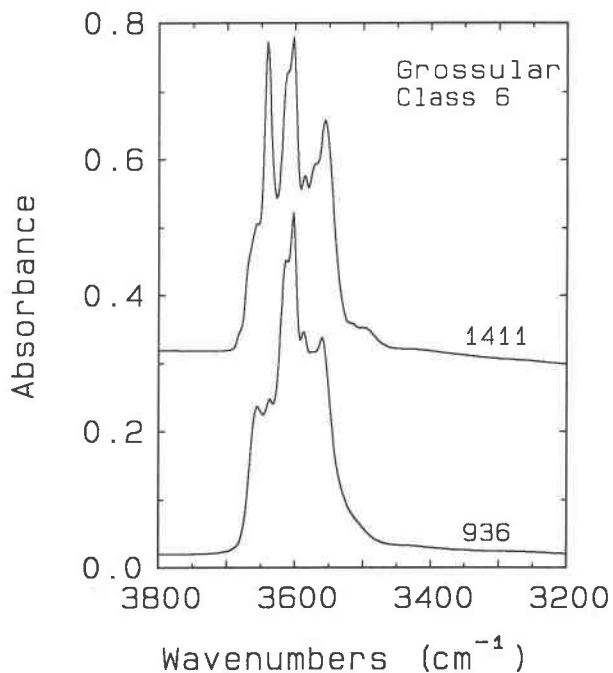


Fig. 9. Class 6 grossular spectra with the strongest peak at 3602 cm^{-1} . From top to bottom: no. 1411, $358\text{ }\mu\text{m}$, Manum; no. 936, $27.2\text{ }\mu\text{m}$, Bric Camula.

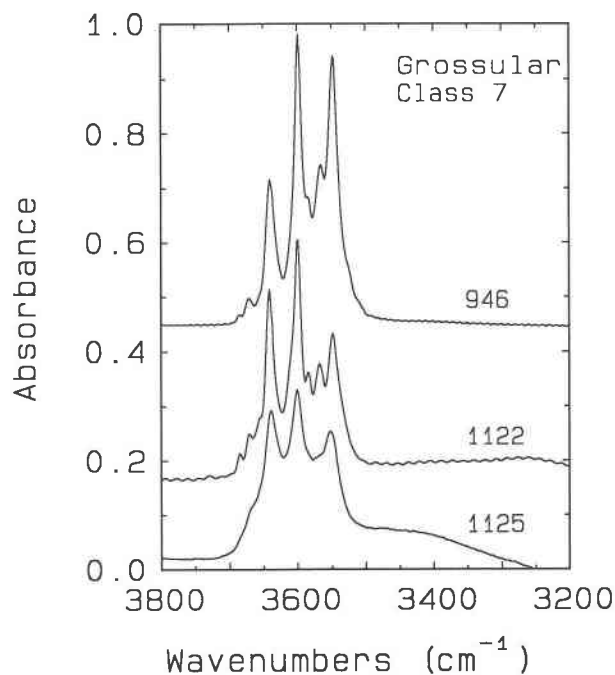


Fig. 10. Class 7 grossular spectra with the strongest peak at 3614 cm^{-1} . From top to bottom: no. 946, $111\text{ }\mu\text{m}$, Auerbach; no. 1122, $175\text{ }\mu\text{m}$, Crestmore; a dark interior zone of no. 1125, 2.812 mm , Lake Jaco.

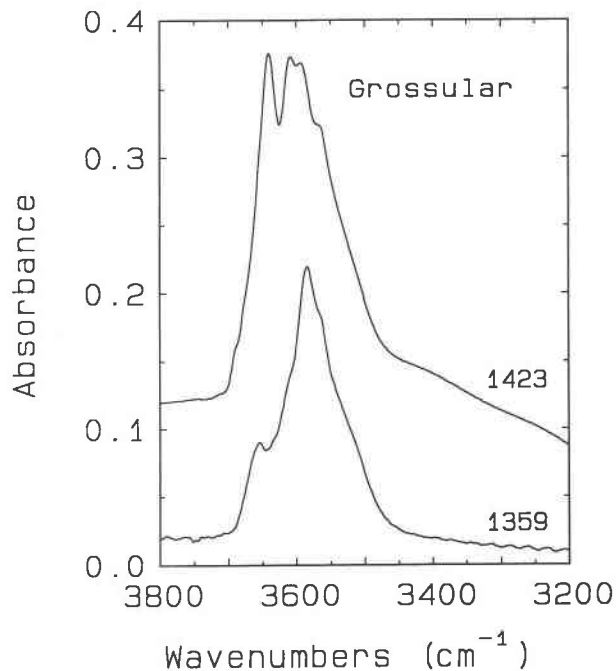


Fig. 11. Grossular spectra that do not fit into one of the spectroscopic classes. From top to bottom: no. 1423, $85.5\text{ }\mu\text{m}$, Oak Grove; no. 1359, $15.0\text{ }\mu\text{m}$, Gruppo di Voltri.

Class 7

Many of the class 2b features are found in these garnet samples. However, the most intense feature of class 7 garnets is the band at about 3599 cm^{-1} (Fig. 10). The 3644 cm^{-1} band of the class 1 garnet samples is replaced by one at 3641 cm^{-1} . These features are found in the spectra of large, orange-brown grossular samples from the contact zone of the calcite body at Crestmore, California, (no. 1122) and Auerbach, Germany, (no. 946) and in the rims of the large grossular samples from skarns east of Lake Jaco, Mexico.

Miscellaneous behavior

Two garnet samples proved difficult to classify into one of the above categories. Their spectra are depicted in Figure 11. The reddish orange grossular from Gruppo di Voltari (no. 1359) has a peak at 3614 cm^{-1} and two prominent side lobes at 3566 and 3658 cm^{-1} .

No evidence of structurally bound molecular H₂O

The near-infrared spectral region was examined for evidence of molecular H₂O in natural garnet. If present, it would give rise to an absorption band at about 5200 cm^{-1} from the combination mode (bend + stretch). Because bands in the region are about 100 times less intense than those in the region of the fundamental stretch of the OH groups ($\sim 3500\text{ cm}^{-1}$), it was necessary to use thick samples for near-infrared studies. When the even less-intense

first overtones of the OH modes were clearly observed near 7100 cm^{-1} , there never was any indication of a H₂O combination mode in the spectra of unaltered, inclusion-free garnet. Our results with grossular samples are consistent with our previous results (Aines and Rossman, 1985b) with pyrope-almandine-spessartine garnets, which also indicated that H substituted in garnets as OH rather than H₂O. The only molecular H₂O found in the garnet spectra is associated with fluid inclusions visible in the sample. In most cases in our study, it was possible to find an optical path sufficiently free of inclusions (e.g., $100\text{ }\mu\text{m}$ diameter) for the spectroscopic measurements.

Zonation of OH

The concentration of OH in these garnets is often heterogeneous. Typical examples are illustrated in Figure 12. There was no consistent zonation trend from core to rim. The rims of grossular samples 1042 (Vesper Peak), 1125 (Lake Jaco), and 1409 (Saline Valley) were most concentrated in OH, whereas the cores of grossular samples 1412 (Mul-Kum) and 1038 (Asbestos) contained the most. The greatest concentration difference we observed was a factor of ~ 4 for grossular sample 1412 from Mul-Kum.

Correlation with chemical composition

We were unable to establish any broadly applicable correlations of individual IR bands with minor or trace components in the garnet samples. Concentration profiles across a number of samples were examined, but they did

not lead to any noteworthy correlations. For example, garnet 1038 contains a green core (Cr^{3+}) and a colorless rim. Although its infrared pattern showed extensive core-to-rim variation, no correlation could be established with major or minor elements.

The large grossular samples from Lake Jaco, Mexico, (e.g., 1125) usually display color zonation. Frequently they have colorless rims with interior zones that are brown when thin. The primary chemical difference between the zones is the order of magnitude greater Ti content in the brown zones. The spectra of the two zones are very different (Fig. 12). Because the spectrum of the dark zone is similar to grossular sample 1122 from Crestmore (Fig. 9), which has about the same Ti content as the colorless zone of the Lake Jaco garnet, it is unlikely that the spectroscopic differences are necessarily due to Ti.

Very little difference results from the substitution of V for Al in grossular from Kenya. The spectrum of the green, vanadian grossular (variety, tsavorite, no. 227) is essentially identical to V-free grossular from the same locality (no. 771) in spite of a large difference in the V content.

The lack of identifiable correlation with the minor element contents was also observed in an extensive study of the zonation of OH in grossular from Belvidere Mountain (Allen and Buseck, 1988). Furthermore, changes in the occupation of the octahedral site had little effect on the spectrum of synthetic high OH-content hydrogrossular samples in the work of Kobayashi and Shoji (1984). They reported that the wavenumbers of OH absorption bands in their synthetic garnet samples changed by only 4–6 cm^{-1} with replacement of up to 10 mol% of andradite.

Temperature dependence of the spectra

The spectra of about one-third of the garnet samples were obtained at ~ 78 K. Spectroscopic resolution improved and more bands were revealed. Although resolution of features improved, the same components could be found in the room temperature spectra with second derivative analysis.

ABSOLUTE H CONTENTS

We have tried to determine the absolute H content of some of these garnet samples with H manometry, evolved H_2O coulometry, and thermal analysis and nuclear reaction analysis. In many instances we find that our results were not reproducible with the low OH-content garnet. In most of these cases, the analyses are being carried out near the limit of their accuracy because of either the low absolute H contents or the difficulty with surface H_2O acquired during the grinding of samples. Furthermore, it is usually necessary to work with very small portions of the sample to avoid the fluid inclusions that are present in nearly all samples. The fluid inclusions have minimal influence upon the spectroscopic results because they occupy a small proportion of the total area of the sample, and it is usually possible to select small apertures to delineate areas free of the inclusions. The inclusions, however, have a major influence upon the total H analyses

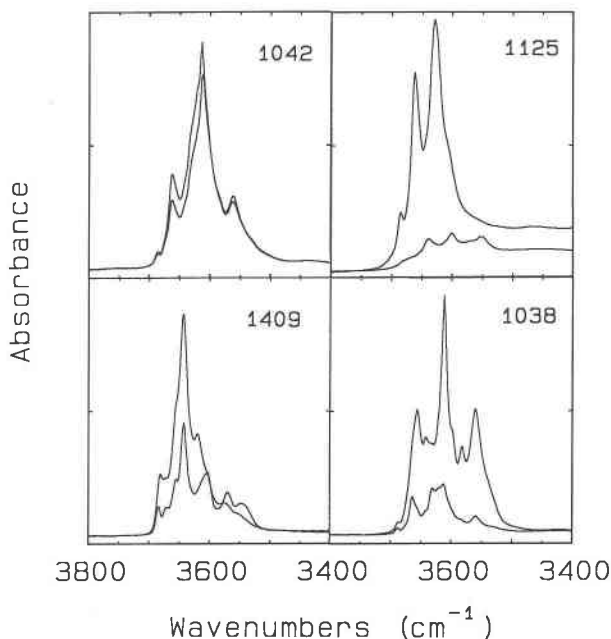


Fig. 12. Four examples of spectra that demonstrate core-to-rim zonation of OH in grossular. Each set of spectra is presented in the 3800 to 3400 cm^{-1} region. No. 1042, Vesper Peak, 1.2 mm thick, 4.0 absorbance full scale, rim slightly more intense than the core. No. 1125, Lake Jaco, 0.60 mm thick, 0.4 absorbance full scale, colorless rim much more intense than the brown core. No. 1409, Saline Valley, 0.18 mm thick, 2.0 absorbance full scale, rim more intense than the core. No. 1038, Asbestos, 0.225 mm thick, 2.0 absorbance full scale, colorless rim less intense than the green core.

because they represent a highly concentrated source of H in the volume of the sample used for H analysis.

Results that we judge to be most reliable are presented in Table 3 together with literature analyses for some of the samples studied. The values believed to be most accurate are from the garnet samples with the highest OH contents. These are used to establish an absolute calibration of the 3600 cm^{-1} region infrared spectral data. Figure 13 summarizes the results. We found that somewhat better correlations can be obtained from integrated absorbance values than from the peak height values (absorbance/millimeter in Table 1).

From the reported OH content of Pabst's Crestmore hydrogrossular (5.88 OH per formula unit) and the OH content of the Crippen hydrogrossular (5.43 OH), we can establish molar absorptivity values for OH in these garnets. The ϵ values per mole per liter concentration of OH calculated from the main peak at about 3598 cm^{-1} are 62 and 79 for the Pabst and Crippen samples, respectively. The integrated absorbance values for these two garnet samples are 3675 and 3816 per mol/L of OH, respectively, where the integrated absorbance is calculated for a crystal 1.0 cm thick.

For purposes of this paper, we use the average integrated

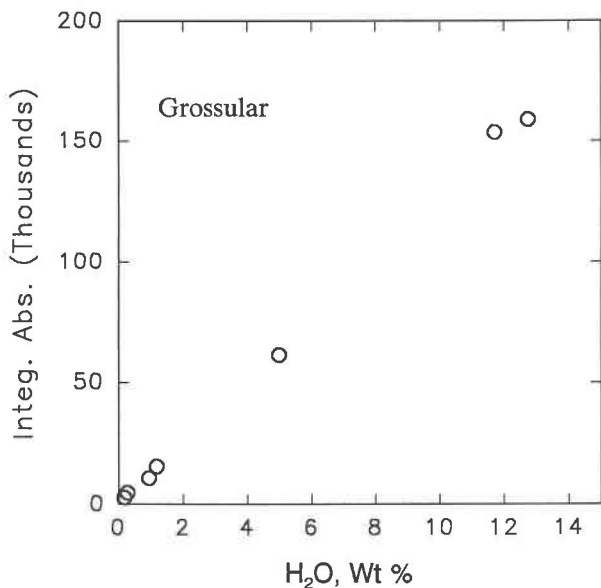


Fig. 13. The calibration of the infrared integrated absorbance in the 3700–3400 cm^{-1} region to analytically determined OH contents expressed as weight percent H_2O .

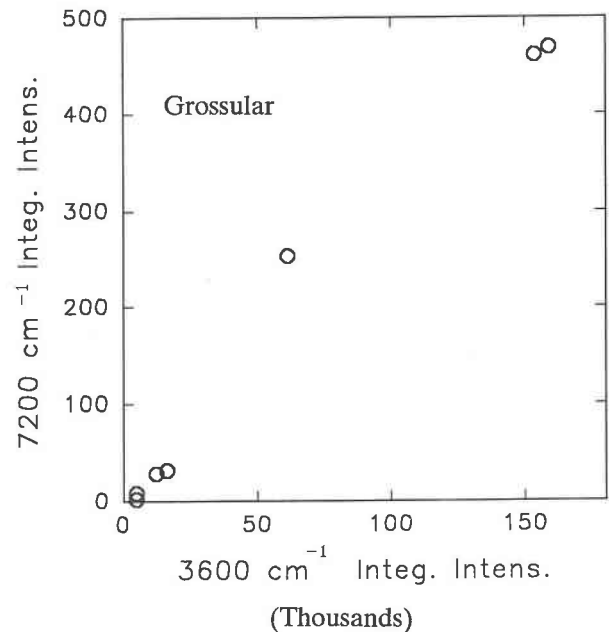


Fig. 14. Correlation between the integrated absorbance in the 3600 cm^{-1} region to the integrated absorbance in the 7200 cm^{-1} region.

absorbance value, 3746, for calculating OH concentrations. Specifically, a crystal 1.5 mm thick with a measured integrated absorbance of 310 would have a calculated integrated absorbance of 2067 for a 1 cm path. This corresponds to an OH concentration of $2067/3746 = 0.546$ mol OH/L. If the crystal's density were 3.15, it would contain $(0.546 \text{ mol/L} \times 17 \text{ g OH/mol}) / (3150 \text{ g/L}) = 0.295$ wt% OH = 0.156 wt% H_2O . The calibration can be expressed in the following two equations:

$$\text{H}_2\text{O wt\%} = 0.0768 (0.0053) \times \text{absorbance per mm}$$

$$\text{H}_2\text{O wt\%} = 0.0000786 (0.0000009)$$

$$\times \text{integrated absorbance per cm}$$

where the numbers in parentheses are the standard error of the coefficient from the regression analysis of the data in Table 3. An integrated absorbance of about 12720 per cm per wt% H_2O is indicated for the higher H_2O content garnets if minor differences in garnet density are ignored.

Many problems and questions remain about the absolute calibration. Our data are inadequate to determine

if the calibration factors actually increase for the low H_2O content garnet samples as the first two points of Figure 13 suggest. We also have not determined if the different classes of hydrogarnet spectra have significantly different calibration factors.

The H_2O contents of our grossular samples range from 12.76% (no. 1329) to nearly zero (no. 1413) with values commonly less than 0.25%. The highest H_2O contents occur in garnets from rodingites, rocks subjected to metasomatic replacement, or from vugs containing products of presumably low-temperature alteration. Garnets from typical carbonate skarns have the lowest H_2O contents.

NEAR INFRARED SPECTRA

In some cases, experimental considerations make it desirable to measure the near-infrared OH overtones at about 7200 cm^{-1} rather than the fundamental bands near 3600 cm^{-1} . We explored the correlation between the intensities

TABLE 3. Summary of calibration data for grossular H_2O analyses

| Garnet | Number | Integ. abs. | H_2O content | Method of analysis |
|----------------|--------|-------------|------------------------------|----------------------------------------|
| Grossular | 53* | 2 877 | 0.18 | P_2O_5 cell coulometry |
| Grossular | 53 | 2 877 | 0.18 | H_2 evolved gas volume |
| Grossular | 53F | 4 796 | 0.28 | ^{19}F nuclear reaction |
| Grossular | 941 | 61 250 | 5.00 | P_2O_5 cell coulometry |
| Hydrogrossular | 1329 | 153 420 | 11.71 | calculated from X-ray a_0 |
| Grossular | 1357 | 15 746 | 1.20 | Basso et al. (1981) |
| Hydrogrossular | 1358 | 158 750 | 12.75 | Basso et al. (1983) |
| Grossular | 1360 | 10 839 | 0.97 | Basso et al. (1984a) |

* Number 13 of Aines and Rossman (1985b).

of the near infrared and the fundamental OH bands. Figure 14 illustrates a good correlation between the integrated intensities of the bands at $\sim 3600\text{ cm}^{-1}$ and $\sim 7200\text{ cm}^{-1}$ in the mid-IR. The peak heights of the $\sim 3600\text{ cm}^{-1}$ bands are about 650 times more intense than those near 7200 cm^{-1} , whereas the integrated intensities are about 340 times greater in the 3600 cm^{-1} region than in the 7200 cm^{-1} region.

The resulting calibration equations are:

$$(\text{H}_2\text{O})\text{ wt\%} = 49.7 (0.78) \times \text{absorbance per mm}$$

$$(\text{H}_2\text{O})\text{ wt\%} = 0.0255 (0.0014)$$

$$\times \text{integrated absorbance per cm}$$

where the numbers in parentheses are the standard error of the coefficient from the regression analysis.

BIREFRINGENT GARNETS

Anisotropic OH absorption was previously reported in a birefringent grossular from Asbestos, Canada, (no. 53) leading Rossman and Aines (1986) to suggest that the ordering of the OH could be responsible for the deviation from cubic symmetry. Three other strongly birefringent garnet samples (nos. 1411 and 1413), including the andradite-grossular from Mul-Kum (no. 1412) described by Hirai and Nakazawa (1986), were examined in this study. The latter three samples differed from the Asbestos garnet by being much more strongly birefringent and by containing much less OH. The latter three garnets have spectra that are only weakly anisotropic in the OH region.

DISCUSSION

The spectra of the natural and synthetic hydrogrossular samples and katoite are most readily interpreted in terms of two types of OH environments that account for the two bands at 3662 cm^{-1} and 3598 cm^{-1} . One pair of candidates for the two sites comes from the X-ray data of Sacerdoti and Passaglia (1985) and Basso et al. (1983) who suggest that the OH sites are different in katoite and plazolite. Sacerdoti and Passaglia have the O-H vector in katoite projecting into the volume of the d-site tetrahedron, whereas Basso et al. (1983) have the O-H vector projecting outside the tetrahedron. This distinction is difficult to support in view of the results of Lager et al. (1987a, 1989) who also find the O-H vector projecting outside the volume of the tetrahedron in both end-member katoite and hydrogrossular samples of intermediate composition.

Hydrogarnet structures display positional disorder that has been described in terms of two O sites (the split-atom model of Ambruster and Lager, 1989). They correspond to the O sites in anhydrous grossular and the sites in Si-free katoite. Our interpretation of the hydrogarnet spectra is that it represents the superposition of these two sites. The 3662 cm^{-1} band in the silica-free hydrogrossular, following the assignment of Harmon et al. (1982), represents O_4H_4 groups that are surrounded by other O_4H_4 groups. The component at 3598 cm^{-1} corresponds to the band in the $3600\text{--}3620\text{ cm}^{-1}$ range previously reported by various

authors. We assign the band at 3598 cm^{-1} , which is dominant in the silica-rich hydrogrossular samples, to (O_4H_4) groups adjacent to SiO_4 groups. The spectrum of the high OH-content hydrogrossular samples then can be viewed as a superposition of the two types of (O_4H_4) components dominated by the Si-free katoite-like sites.

The hydrogrossular spectrum in common garnet

The spectra of most of the low OH content, macroscopic grossular samples do not resemble those of garnets with verified hydrogrossular substitution. Only the class 4 spectra resemble the spectra of the authentic intermediate SiO_4 content hydrogrossulars. The complexity and diversity of the spectra of the low OH content grossular argue that the hydrogrossular substitution found in the high OH content garnets is not the dominant mode of substitution at lower OH contents.

A number of authors have proposed that H occupies sites other than the tetrahedral Si site in hydrogarnets. Basso et al. (1984a, 1984b), Basso and Cabella (1990), and Birkett and Trzcienski (1984) proposed that H may substitute in both the dodecahedral and octahedral sites. Kalinichenko et al. (1987) suggest that the protons in hydrogrossular are situated in both the tetrahedral and the octahedral sites. The complexity of the spectra of low OH content grossular in the OH region is intuitively consistent with a multiple site occupancy. However, an attempt by Lager et al. (1989) to test this hypothesis found no evidence for multisite occupancy in the X-ray study of hydrogrossular titanian andradites. Unfortunately, the garnets that often show the greatest spectral complexity in the OH region contain concentrations of OH too low to be studied by conventional diffraction techniques. Our initial attempts to examine this problem with NMR methods have also been thwarted by the low OH concentrations in most natural samples (Yesinowski et al., 1988).

CONCLUSIONS

1. Essentially all grossular contains OH.
2. The fine-grained grossular samples classically called hydrogrossular are the most OH-rich.
3. Among macroscopic grossular, that from rodingites is the richest in the OH component.
4. Garnets from carbonate skarns contain the lowest concentrations of OH.
5. The OH is readily observed in infrared spectra.
6. The infrared spectra of macroscopic garnet samples are significantly different from the spectra of true hydrogrossular, suggesting that the hydrogarnet substitution $\text{SiO}_4 = (\text{O}_4\text{H}_4)$ is not the only means of incorporating OH.
7. For macroscopic grossular examined in this study, seven different classes of infrared spectra can be identified based on the energy of the most intense OH absorption band.
8. Grossular can be zoned in both the concentration of OH and in details of its site in the crystal.
9. The details of the OH absorption in the infrared are

so characteristic that in many cases it was possible to identify the locality from which an individual grossular came once a standard spectrum was available.

10. The analytical amount of OH in grossular can be estimated from the infrared spectrum. An integrated absorbance of 3746 per cm thickness corresponds to an OH concentration expressed as H₂O of 1 mol of H₂O per liter of sample.

ACKNOWLEDGMENTS

We thank D.G. Schlom for assisting with our synthesis of hydrogarnet and G.A. Lager (University of Kentucky) for providing samples of his synthetic hydrogarnets and numerous helpful discussions about the hydrogarnet substitution. Other garnets for this study were donated by A.L. Albee (Caltech), F.M. Allen (Arizona State University), G. Amthauer (Salzburg), D. Atkinson (Santa Barbara), R. Basso (Genoa), C. Bridges (Nairobi), B. Cannon (Seattle), R. Coleman (Stanford), R.H. Currier (Arcadia), P. Flusser (Los Angeles), C. Francis (Harvard Mineral Museum), M. Gray (Culver City), G. Harlow (American Museum), W.A. Henderson (Stanford), H.S. Hill (Altadena), P. Keller (Los Angeles County Museum), G.A. Novak (California State University, Los Angeles), and Y. Takeuchi (Tokyo). This study was funded in part by NSF grants EAR-7919987, EAR-8313098, EAR-8618200, and EAR-8916064. Contribution no. 4449.

REFERENCES CITED

- Aines, R.D., and Rossman, G.R. (1985a) The water content of mantle garnets. *Geology*, 12, 720–723.
- (1985b) The hydrous component in garnets: Pyrospites. *American Mineralogist*, 69, 1116–1126.
- Allen, F.M., and Buseck, P.R. (1988) XRD, FTIR, and TEM studies of optically anisotropic grossular garnets. *American Mineralogist*, 73, 568–584.
- Armbruster, T., and Lager, G.A. (1989) Oxygen disorder and the hydrogen position in garnet-hydrogarnet solid solutions. *European Journal of Mineralogy*, 1, 363–369.
- Bank, H. (1982) Über Grossular und Hydrogrossular. *Zeitschrift der Deutschen Gemmologischen Gesellschaft*, 31, 93–96.
- Basso, R., and Cabella, R. (1990) Crystal chemical study of garnets from metarodingites in the Voltri Group metaophilites (Ligurian Alps, Italy). *Neues Jahrbuch für Mineralogie Monatshefte*, 127–136.
- Basso, R., Giusta, A.D., and Zefiro, L. (1981) A crystal structure study of a Ti-containing hydrogarnet. *Neues Jahrbuch für Mineralogie Monatshefte*, 230–236.
- (1983) Crystal structure refinement of plazolite: A highly hydrated natural hydrogrossular. *Neues Jahrbuch für Mineralogie Monatshefte*, 251–258.
- Basso, R., Cimmino, F., and Messiga, B. (1984a) Crystal chemical and petrological study of hydrogarnets from a Fe-gabbro metarodingite (Gruppo di Voltri, Western Liguria, Italy). *Neues Jahrbuch für Mineralogie Abhandlung*, 150, 247–258.
- (1984b) Crystal chemistry of hydrogarnets from three different microstructural sites of a basaltic metarodingite from the Voltri Massif (Western Liguria, Italy). *Neues Jahrbuch für Mineralogie Abhandlung*, 148, 246–258.
- Birkett, T.C., and Trzcinski, W.E. (1984) Hydrogarnet: Multi-site hydrogen occupancy in the garnet structure. *Canadian Mineralogist*, 22, 675–680.
- Cohen-Addad, C., Ducros, P., and Bertaut, E.F. (1967) Etude de la substitution du groupement SiO₄ par (OH)₄ dans les composés Al₂Ca₃(OH)₁₂ et Al₂Ca₃(SiO₄)_{2,16}(OH)_{3,36} de type grenet. *Acta Crystallographica*, 23, 220–230.
- Foreman, D.W. (1968) Neutron and X-ray diffraction study of Ca₃Al₂(O₄D)₃, a garnetoid. *Journal of Chemical Physics*, 48, 3037–3041.
- Foshag, W.F. (1920) Plazolite, a new mineral. *American Mineralogist*, 5, 183–185.
- Frankel, J.J. (1959) Uvarovite garnet and South African jade from Transvaal. *American Mineralogist*, 44, 565–591.
- Harmon, K.H., Gabriele, J.M., and Nuttall, A.S. (1982) Hydrogen bonding. Part 14. Hydrogen bonding in the tetrahedral O₄H₄⁺ cluster in hydrogrossular. *Journal of Molecular Structure*, 82, 213–219.
- Hirai, H., and Nakazawa, H. (1986) Visualizing low symmetry of a grandite garnet on precession photographs. *American Mineralogist*, 71, 1210–1213.
- Hsu, L.C. (1980) Hydration and phase relations of grossular-spessartine garnets at P_{H₂O} = 2Kb. *Contributions to Mineralogy and Petrology*, 71, 407–415.
- Kalinichenko, A.M., Proshko, V.Ya., Matyash, I.C., Pavlishin, V.I., and Gamarnik, M.Ya. (1987) NMR data on crystallochemical features of hydrogrossular. *Geochemistry International*, 24, 132–135 (translated from *Geokhimiya*, no. 9, 1363–1366, 1986).
- Kobayashi, S., and Shoji, T. (1983) Infrared analysis of the grossular-hydrogrossular series. *Mineralogical Journal*, 11, 331–343.
- (1984) Infrared analysis of the grossular-hydrogrossular series with a small amount of andradite molecule. *Mineralogical Journal*, 12, 122–136.
- Lager, G.A., Armbruster, T., and Faber, J. (1987a) Neutron and X-ray diffraction study of hydrogarnet Ca₃Al₂(O₄H₄). *American Mineralogist*, 72, 756–765.
- Lager, G.A., Rossman, G.R., Rotella, F.J., and Schultz, A.J. (1987b) Neutron-diffraction structure of a low-water grossular at 20 K. *American Mineralogist*, 72, 766–768.
- Lager, G.A., Armbruster, T., Rotella, F.J., and Rossman, G.R. (1989) The OH substitution in garnets: X-ray and neutron diffraction, infrared and geometric-modeling studies. *American Mineralogist*, 74, 840–851.
- Pabst, A. (1937) The crystal structure of plazolite. *American Mineralogist*, 22, 861–868.
- Passaglia, E., and Rinaldi, R. (1984) Katoite, a new member of the Ca₃Al₂(SiO₄)-Ca₃Al₂(OH)₁₂ series and a new nomenclature for the hydrogrossular group of minerals. *Bulletin de Minéralogie*, 107, 605–618.
- Rinaldi, R., and Passaglia, E. (1989) Hibschite topotype: Crystal chemical characterization. *European Journal of Mineralogy*, 1, 639–644.
- Rossman, G.R., and Aines, R.D. (1986) Birefringent grossular from Asbestos, Quebec, Canada. *American Mineralogist*, 71, 779–780.
- Sacerdoti, M., and Passaglia, E. (1985) The crystal structure of katoite and implications within the hydrogrossular group of minerals. *Bulletin de Minéralogie*, 108, 1–8.
- Wilkins, R.W.T., and Sabine, W. (1973) Water content of some nominally anhydrous silicates. *American Mineralogist*, 58, 508–516.
- Woodward, A.O., Crippen, R.A., and Garner, K.B. (1941) Section across Commercial Quarry, Crestmore, California. *American Mineralogist*, 26, 351–381.
- Yesinowski, J.P., Eckert, H., and Rossman, G.R. (1988) Characterization of hydrous species in minerals by high-speed ¹H MAS-NMR. *Journal of the American Chemical Society*, 110, 1367–1375.
- Zabinski, W. (1966) Hydrogarnets. *Polska Akademia Nauk, Oddzial Krakow, Komisja Nauk Mineralogicznych, Prace Mineralogiczne*, 3, 1–69.

MANUSCRIPT RECEIVED AUGUST 20, 1990

MANUSCRIPT ACCEPTED APRIL 18, 1991